DOI: 10.1002/chem.201003157

Synthesis and Binding Studies of Novel Diethynyl-Pyridine Amides with Genomic Promoter DNA G-Quadruplexes

Jyotirmayee Dash,*[a, b] Zoë A. E. Waller,[a, c] G. Dan Pantoş,[a, f] and Shankar Balasubramanian*[a, d, e]

Abstract: Herein, we report the design, synthesis and biophysical evaluation of novel 1,2,3-triazole-linked diethynyl-pyridine amides and trisubstituted diethynyl-pyridine amides as promising G-quadruplex binding ligands. We have used a Cu^{I}-catalysed azide–alkyne cycloaddition click reaction to prepare the 1,2,3-triazole-linked diethynyl-pyridine amides. The G-quadruplex DNA binding properties of the ligands have been examined by using a Förster resonance energy transfer (FRET) melting assay and surface plasmon resonance (SPR) experiments. The investigated compounds are conformationally flexible, having free rotation around the triple bond, and exhibit enhanced G-quadruplex binding stabilisation and specificity between intramolecular promoter G-quadruplex DNA motifs compared to the first generation of diarylethynyl amides (*J. Am. Chem. Soc.* **2008**, *130*, 15950–15956). The ligands show versatility in molecular recognition and promising G-quadruplex discrimination with 2–50-fold selectivity exhibited between different intramolecular promoter G-quadruplexes. Circular dichroism (CD) spectroscopic analysis suggested that at higher concentration these ligands disrupt the c-kit2 G-quadruplex structure. The studies validate the design concept of the 1,3-diethynyl-pyridine-based scaffold and demonstrate that these ligands exhibit not only significant selectivity over duplex DNA but also variation in G-quadruplex interaction properties based on small chemical changes in the scaffold, leading to unprecedented differential recognition of different DNA G-quadruplex sequences.

Keywords: acetylene · amides · click chemistry · G-quadruplexes · molecular recognition

Introduction

G-quadruplex DNA structural motifs have been identified as potential anticancer drug targets.[1] Bioinformatics studies revealed the prevalence of G-quadruplex-forming sequences in the human genome, and particularly in promoter regions.[2] It has been proposed that they might play important roles in regulating oncogenic expression of certain oncogenes, such as c-myc,[3] c-kit[4] and k-ras.[5]

Most of the first generation G-quadruplex ligands comprise a planar, aromatic core presumed to stack on the terminal tetrads of the G-quadruplex.[6,7] Some of these ligands show good selectivity for G-quadruplex DNA over duplex DNA.[6,7] All G-quadruplex structures share a common G-quartet structural feature, but vary in their respective sequences and loop length, which provides an opportunity to achieve specificity in molecular recognition by using the hyper-variable loops and the groove regions. Recently, the goal of achieving differential recognition of G-quadruplex DNA by small molecule ligands has received considerable interest[8,9] and we have been evaluating classes of ligands for different G-quadruplex DNA targets.[8,9]

We have recently reported G-quadruplex recognition by two novel G-quadruplex binding ligands based on bis(phenylenethynyl) amides (**1** and **2**),[9b] containing *N*,*N*-dimethylpropylamine side chains. We found that ligand **2**, with a central pyridine ring, shows higher stabilisation potential and binding affinities for G-quadruplex DNA compared to the

[a] Dr. J. Dash, Dr. Z. A. E. Waller, Dr. G. D. Pantoş, Prof. Dr. S. Balasubramanian
Department of Chemistry, University of Cambridge
Lensfield Road, Cambridge CB2 1EW (UK)
Fax: (+44) 1223-336-913
E-mail: sb10031@cam.ac.uk

[b] Dr. J. Dash
Department of Chemical Sciences
Indian Institute of Science Education and Research-Kolkata, Mohanpur Campus
Mohanpur 7412 52, Nadia, West Bengal (India)
Fax: (+91) 33-25873020
E-mail: jyotidash@iiserkol.ac.in

[c] Dr. Z. A. E. Waller
School of Pharmacy, University of East Anglia
Norwich, NR4 7TJ (UK)

[d] Prof. Dr. S. Balasubramanian
Cancer Research UK, Cambridge Research Institute
Li Ka Shing Center, Cambridge, CB2 0RE (UK)

[e] Prof. Dr. S. Balasubramanian
School of Clinical Medicine, University of Cambridge
Cambridge, CB2 0SP (UK)

[f] Dr. G. D. Pantoş
Department of Chemistry, University of Bath
Bath, BA2 7AY (UK)

Supporting information for this article is available on the WWW under http://dx.doi.org/10.1002/chem.201003157.

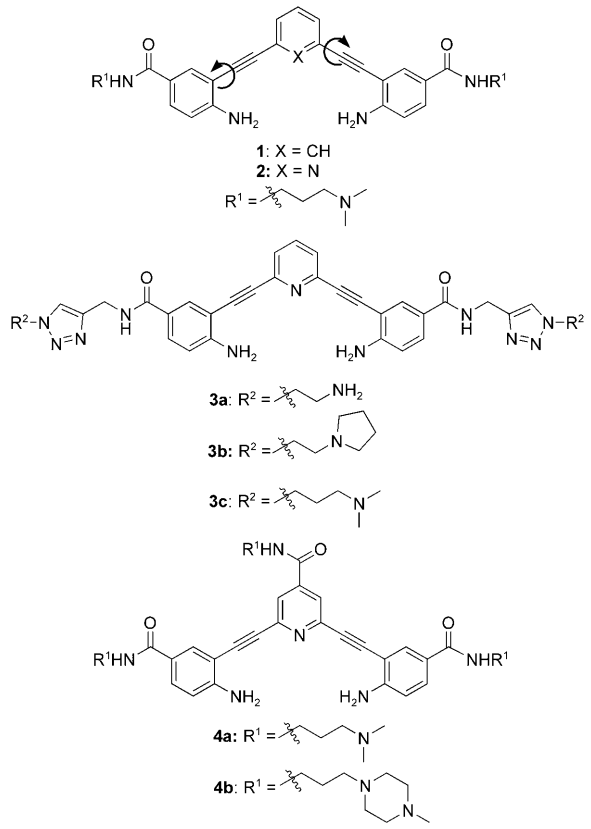

benzene analogue **1** and thus, offers an attractive template for ligand design. These compounds are conformationally flexible, as they possess the ability for free rotation around the triple bond. In order to achieve enhanced binding ability and differential recognition of this class of molecules towards diverse G-quadruplex sequences we planned to improve the binding properties of the first generation molecule **2** with the synthesis of substituted ligands of the 1,3-diethynyl pyridine scaffold (e.g., 1,4-triazole-linked amides **3** and trisubstituted amides **4**). The heteroaromatic 1,4-substituted 1,2,3-triazole ring system has attracted extensive interest owing to its wide use as a synthetic building block endowed with pharmacological potential.[10] The incorporation of this triazole unit has also been reported to enhance G-quadruplex stabilisation and selectivity.[11] We considered that linking the heteroaromatic 1,4-substituted 1,2,3-triazole ring into the adaptive core of the 1,3-diethynyl pyridine scaffold may improve the ability of such molecules to interact specifically with G-quadruplex DNA, making them attractive probes for the investigation of the biological function of G-quadruplexes. Furthermore, we have designed trisubstituted ligands **4** wherein the side chains can target the hypervariable loops and grooves that distinguish each G-quadruplex, thereby providing the potential for G-quadruplex discrimination.

Results and Discussion

Synthesis: Ligands **3a–c** were synthesised by using a sequence of two chemoselective reactions, amide coupling of diacid **8** and Cu^{I}-catalysed Huisgen cycloaddition of bisamide **9** (Scheme 1).[10] The diacid **8** was prepared by using

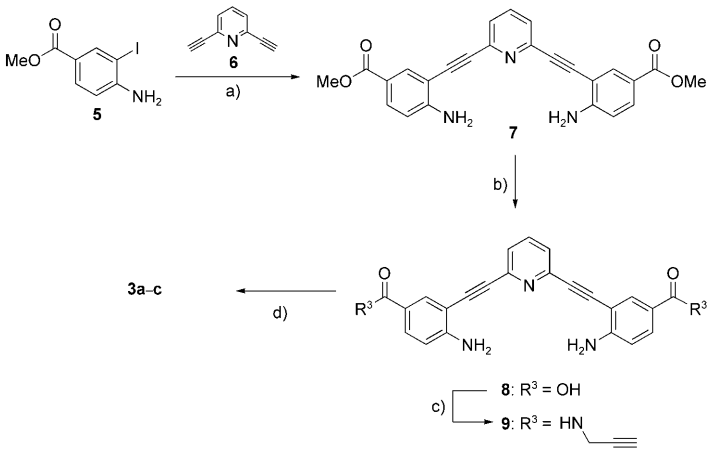

Scheme 1. Synthesis of triazole-linked ligands **3a–c**. a) $[PdCl_2(PPh_3)_2]$, CuI, Et_3N, DMF, RT, 7 h, 83%; b) NaOH (2N), THF/MeOH (1:1), RT, 12 h, 91%; c) propargylamine, *N'*-(3-dimethylaminopropyl)-*N*-ethylcarbodiimide (EDC), 1-hydroxybenzotriazole (HOBt), *N*-methylmorpholine (NMM), DMF, RT, 10 h; d) R^2–N_3 (**10a–c**), $CuSO_4 \cdot 5H_2O$, sodium ascorbate, *t*BuOH/H_2O (1:1), RT, 12 h, 71–75% from **8**.

our previously reported procedure, starting from the iodoaniline derivative **5** and 2,6-diethynylpyridine (**6**).[9b] The diacid **8** was coupled with propargylamine by using EDC, HOBT and NMM in DMF to give the amide derivative **9**, which was directly used without any further purification. The azides **10a–c** were prepared from the corresponding –halides (see the Supporting Information). The target ligands **3a–c** were synthesised selectively from tetra-alkyne **9** and the azide building blocks **10a–c** by copper(I)-catalysed click chemistry. Under copper(I)-catalysed azide–alkyne Huisgen cycloaddition conditions the terminal alkyne units of intermediate **9** selectively reacted with the azides **10**. The desired 1,4-substituted 1,2,3-triazole-linked products **3a–c** were obtained from **8** with yields of 71–75% (Scheme 1). Each ligand was purified by preparative HPLC to afford samples of suitable purity for biophysical evaluation.

Methyl 2,6-diethynylisonicotinate (**12**) was obtained in two steps through Pd-catalysed Sonogashira coupling of methyl 2,6-dichloroisonicotinate (**11**) with trimethylsilylacetylene and removal of the silyl protecting groups by tetrabuylammonium fluoride (TBAF) (Scheme 2).[12] Palladium-catalysed cross-coupling of **12** with iodoaniline derivative **5** gave the desired triester derivative in 73% yield. Basic hydrolysis of **13** afforded triacid **14** in near quantitative yield. The triacid **14** was treated with the corresponding amine derivatives **15a** and **15b** to give ligands **4a** and **4b** in 81–84% yield (Scheme 2).

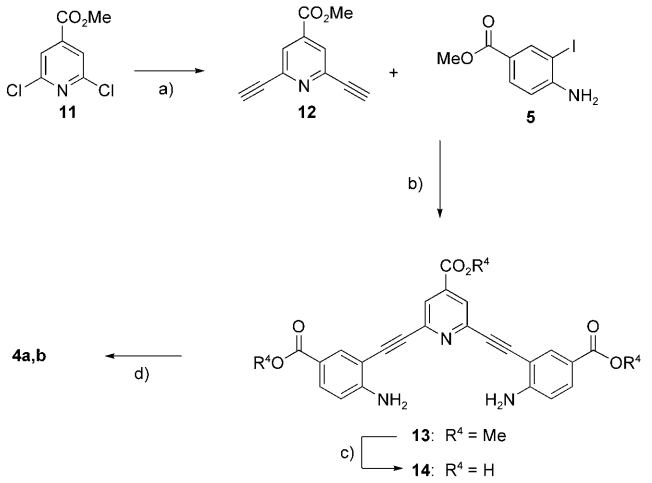

Scheme 2. Synthesis of trisubstituted ligands. a) i) Trimethylsilylacetylene, $[Pd_2(dba)_3]$ (dba = dibenzylideneacetone), PPh_3, CuI, Et_3N, 60°C; ii) TBAF, THF, −30°C, 5 min, 91%; b) $[PdCl_2(PPh_3)_2]$, CuI, Et_3N, DMF, RT, 7 h, 73%; c) NaOH (2N), THF/MeOH (1:1), RT, 12 h, 99%; d) R^1–NH_2 (**15a,b**), EDC, HOBt, NMM, DMF, RT, 10 h, 81–84%.

Small molecule–DNA interactions: Small molecule–quadruplex DNA recognition was evaluated by using Förster resonance energy transfer (FRET)[13] melting and surface plasmon resonance (SPR)[14] experiments. Our studies have focused on the binding of small molecules to four biologically relevant distinct G-quadruplexes derived from sequences found in the promoter of the proto-oncogenes k-ras, c-myc and c-kit (which has two quadruplex forming sequences: c-kit1 and c-kit2) and a double stranded (ds) DNA control.

FRET melting analysis: FRET melting analysis[13] has been used to determine the G-quadruplex stabilisation and selectivity of a ligand series towards a particular G-quadruplex target.[8,9,13] Because each DNA target exhibits a different melting temperature (T_m) value, the selectivity between two different quadruplex targets cannot be directly compared by using shifts in T_m values (ΔT_m). From FRET melting experiments that use dual-labelled sequences (see the Experimental Section) we found that ligands **3** and **4** show enhanced stabilisation potential (i.e., a positive ΔT_m) compared to the parent ligand **2**. The results are summarised in Table 1 and thermal shift profiles of ligands **3** and **4** are depicted in Figure 1.

Table 1. G-quadruplex stabilisation (ΔT_m) potential determined by FRET melting analysis.[a]

Ligand	ΔT_m at 1 μM concentration [K]				
	k-ras	c-myc	c-kit1	c-kit2	ds
2	12.2	7.3	13.5	9.2	0.2
3a	17.1	11.8	20.0	16.5	0.7
3b	14.8	10.4	17.5	12.7	0.6
3c	16.0	10.1	18.4	14.5	0.0
4a	33.0	17.0	31.3	21.8	1.0
4b	29.4	16.7	27.5	18.2	1.8

[a] The T_m values of the quadruplexes in 60 mM potassium cacodylate buffer, pH 7.4 in the absence of ligands are: k-ras (46±1), c-myc (77±1), c-kit1 (57±1), c-kit2 (71±1), ds DNA (58±1)°C; maximum measurable T_m = 95°C.

Small molecules **3a** and **4a** were found to be significantly more selective for G-quadruplexes compared to duplex DNA. In the bis-triazole ligand series, **3a** with primary amino groups showed improved G-quadruplex DNA stabilisation over **3b**, which possesses pyrrolidino terminal substituents. Ligand **3c** with *N,N*-dimethylaminopropyl side chains exhibited comparable stabilisation temperatures to ligands **3a** and **3b**, indicating that stabilising properties are not adversely affected by slight modification of chain length. Overall the bis-triazole amide **3a** exhibited good stabilisation potentials with ΔT_m values at 1 μM ligand concentration of 17.1, 11.8, 20.0 and 16.5 K for k-ras, c-myc, c-kit1 and c-kit2 G-quadruplexes, respectively.

The trisubstituted ligand **4a** shows higher stabilisation potentials for all the quadruplex DNA sequences tested than observed for ligands **2** and **3**. Ligand **4a** with *N,N*-dimethyl amino side chains showed relatively higher stabilisation compared to ligand **4b** with *N*-methylpiperazinyl amino side chains. It is noteworthy that ligand **4a** is the best G-quadruplex DNA stabilising ligand in the series, and showed ΔT_m near to the maximum that can be measured by this method for c-myc and c-kit2 G-quadruplexes (ΔT_m = 17.0 and 21.8 K, respectively, i.e., a T_m of 94°C at 1 μM ligand concentration). Ligand **4a** also showed stronger stabilisation for k-ras (ΔT_m = 33.0 K) and c-kit1 (ΔT_m = 31.3 K) G-quadruplex DNA at 1 μM concentration. Whereas the parent 1,3-diethynyl pyridine bis-amide **2** exhibited a relatively low stabilisation potential with ΔT_m values of 12.2, 7.3, 13.5 and 9.2 K for k-ras, c-myc, c-kit1 and c-kit2, respectively, the triazole-linked ligands **3** and the trisubstituted ligands **4** significantly increase the stabilisation potential and selectivity for a particular quadruplex target.

SPR binding analysis and selectivity: Surface plasmon resonance can be employed to measure kinetics and equilibrium binding constants[14] and has been used to determine the selectivity of small molecule ligands for binding different G-quadruplex sequences.[8,9] SPR data reveal that these ligands exhibit a wide range of binding affinities and selectivity for different G-quadruplex sequences. The correlation between stabilisation (ΔT_m) and equilibrium binding (K_d) is not straightforward and thus, there is no simple relationship between ΔT_m and K_d. The results are reported in Table 2 and binding curves are depicted in Figure 2 (see the Supporting Information). Ligand **3a** with triazole linkers showed a preference of at least an order of magnitude for the c-kit1 quad-

Table 2. Dissociation constants (K_d) measured by SPR.

Ligand	K_d [μM]				
	k-ras	c-myc	c-kit1	c-kit2	ds
2	1.2±0.1	0.57±0.02	3.04±0.08	0.69±0.03	[a]
3a	0.74±0.05	0.35±0.02	0.35±0.03	0.20±0.06	[a]
3b	8.9±3.4	2.5±0.1	2.8±0.6	1.9±0.1	[a]
3c	19±0.5	0.36±0.02	0.47±0.04	1.8±0.7	[a]
4a	0.21±0.1	0.43±0.02	0.40±0.03	0.12±0.03	[a]
4b	9.4±1.6	0.91±0.03	1.6±0.3	2.1±0.9	[b]

[a] No significant binding up to 25 μM. [b] Non-specific interaction.

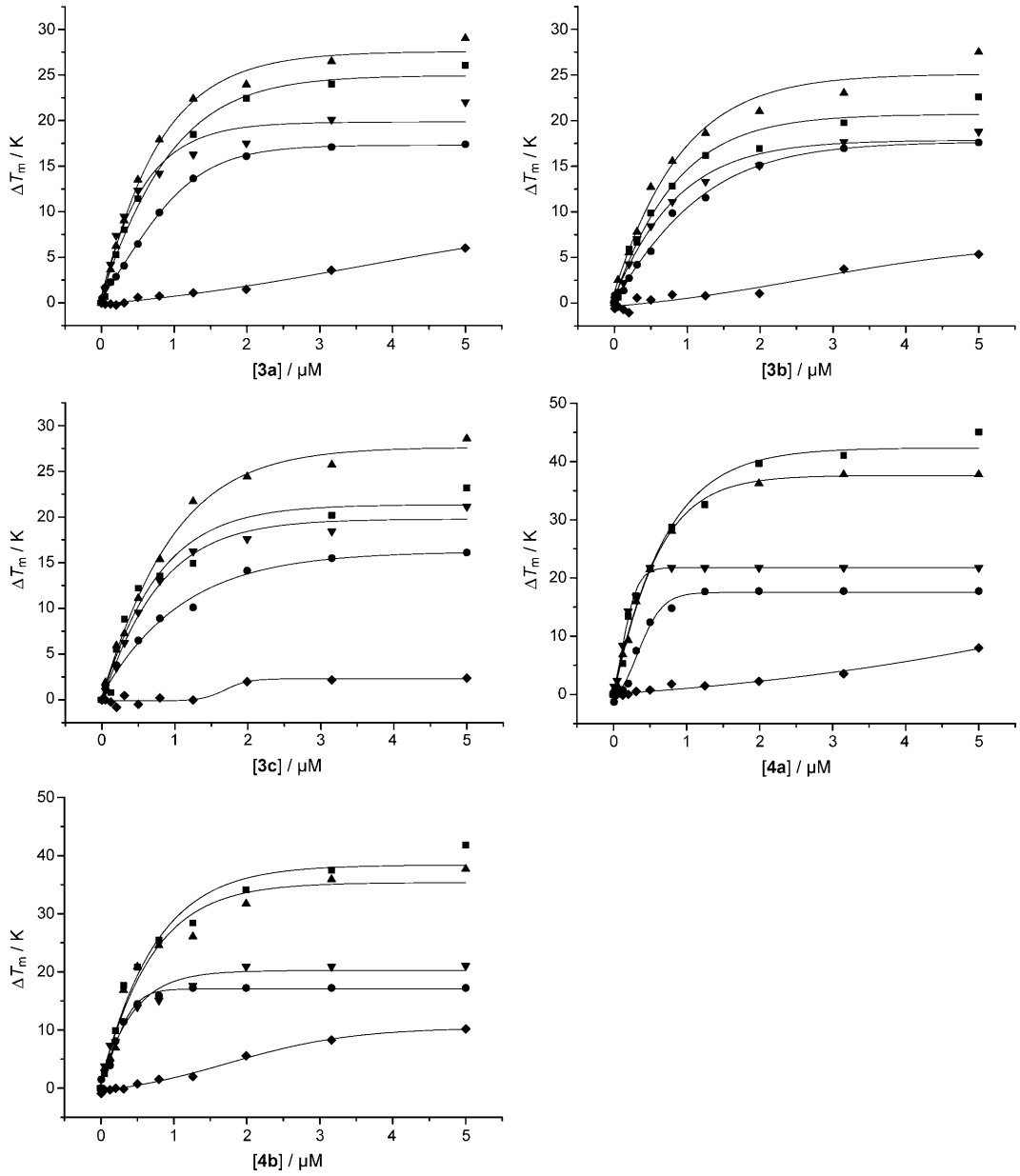

Figure 1. FRET stabilisation curves for ligands **3** and **4** (■ = k-ras, ● = c-myc, ▲ = c-kit1, ▼ = c-kit2, ◆ = ds DNA).

ruplex compared to the parent ligand **2**. Ligands **3a**–**c** did not show much discrimination between c-myc and c-kit1 G-quadruplexes, but the compounds showed strong binding affinity for both sequences. In agreement with the FRET melting experiments, ligand **3a**, which contains free amino side chains, showed not only high stabilisation potentials (Table 1) but also exhibits correspondingly high binding affinities (Table 2) compared to ligands **3b** and **3c**. Ligand **3a** and **3b** each show 3–5-fold selectivity for the c-kit2 over the k-ras quadruplex. Ligand **3c** showed high binding affinity towards the c-myc and c-kit1 quadruplexes with submicromolar equilibrium dissociation constants (K_d) of 360 and 470 nM, respectively, and with a modest K_d (1.8 μM) for c-kit2 and high K_d (19 μM) for k-ras. It is intriguing to note that ligand **3c** showed a preference for the c-myc and the c-kit1 G-quadruplex sequences, exhibiting 4–6-fold selectivity for c-myc and c-kit1 over c-kit2 and a 40–50-fold preference for c-myc and c-kit1 over the k-ras quadruplex (Table 2, Figure 2). To the best of our knowledge, this is one of the highest levels of discrimination reported by a small molecule ligand between intramolecular promoter quadruplexes.

Ligand **4a** showed 5–7-fold improvement in binding affinity compared to the parent molecule **2** for the k-ras, c-kit1 and c-kit2 quadruplexes. Ligand **4a** exhibited a preference for the c-kit2 quadruplex (K_d = 120 nM) over the k-ras (K_d = 210 nM), c-myc (K_d = 430 nM) and c-kit1 (K_d = 400 nM) quadruplexes. Ligand **4a** was found to have the strongest binding affinity for the c-kit2 quadruplex and also exhibits higher

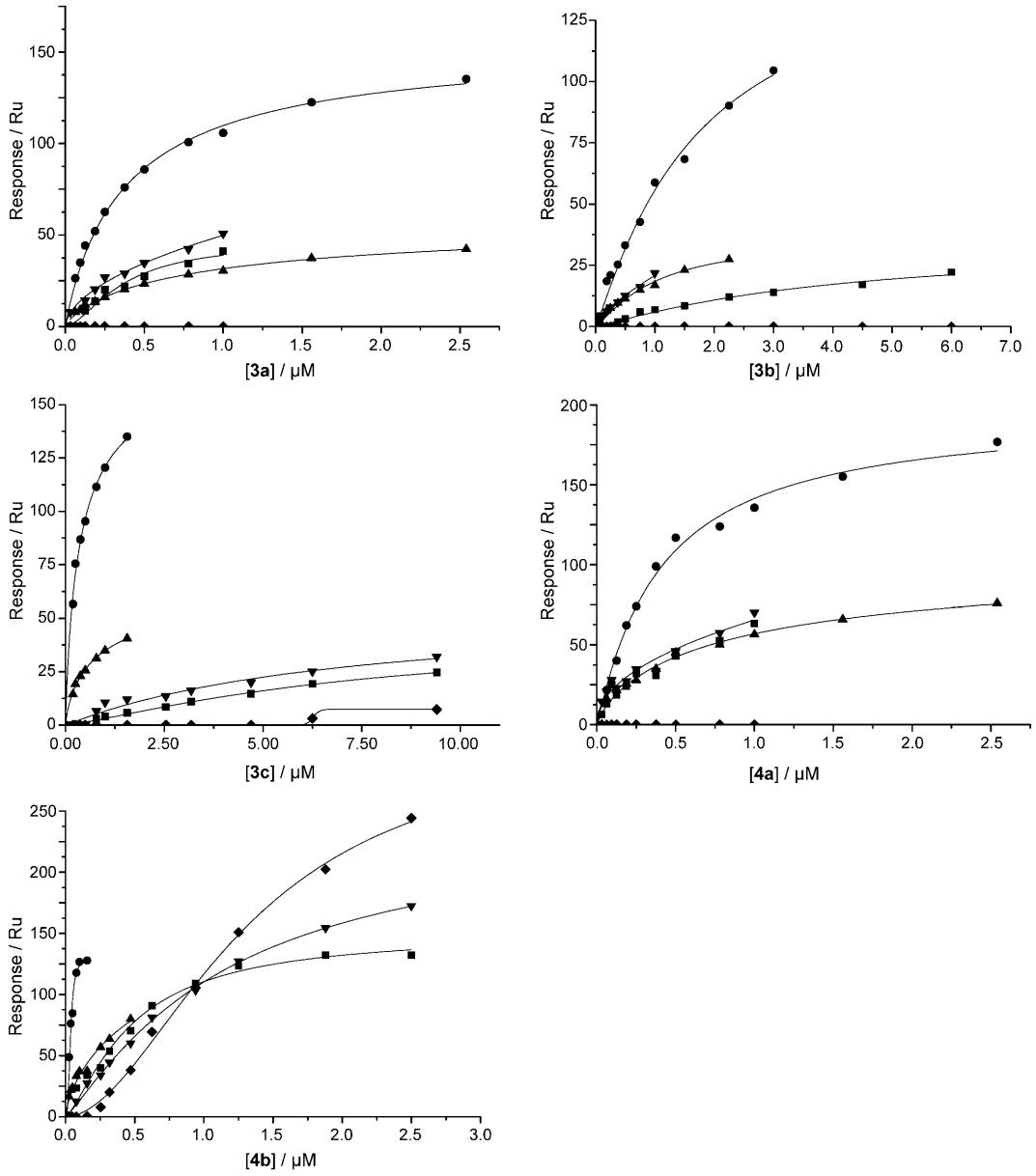

Figure 2. SPR binding curves for ligands **3** and **4** (■ = k-ras, ● = c-myc, ▲ = c-kit1, ▼ = c-kit2, ◆ = ds DNA).

binding affinity compared to ligand **4b**. Ligand **4a** shows a discrimination of 2–4-fold among the intramolecular quadruplexes examined in the study (Table 2). Ligand **4b** showed a preference for the c-myc quadruplex with a submicromolar K_d of 910 nM (Table 2). Despite this, the ligand demonstrated evidence of non-specific interactions with duplex DNA (Figure 2, **4b**, see the Supporting Information), suggestive of multiple binding sites associated with electrostatic aggregation. These results are indicative that the addition of the piperazino functionality increases non-specific electrostatic interactions with DNA (see the Supporting Information).

Circular dichroism (CD) spectroscopic studies: CD spectroscopy has been used to understand fundamental properties of G-quadruplex recognition and binding modes of ligands.[15,16] We used CD spectroscopy to examine the effects of two high-affinity ligands, **3a** and **4a**, on c-kit2 G-quadruplex DNA in the presence and absence of stabilising salt. The CD spectrum of c-kit2 suggests that in the absence of any added salt c-kit2 exists as a mixture of a parallel structure (a positive peak at 260 nm) and an antiparallel conformation (a minor peak at 295 nm).[4a] We have reported that small molecule **2** templates the folding of the c-kit2 quadruplex into the parallel conformation in the absence of any added salt.[9b] Similarly, we found that ligand **3a** and **4a** induce folding of the c-kit2 quadruplex to a parallel structure (Figure 3 A and B). Upon each addition of ligand **3a** or **4a** to the c-kit2 quadruplex there is an increase in ellipticity at

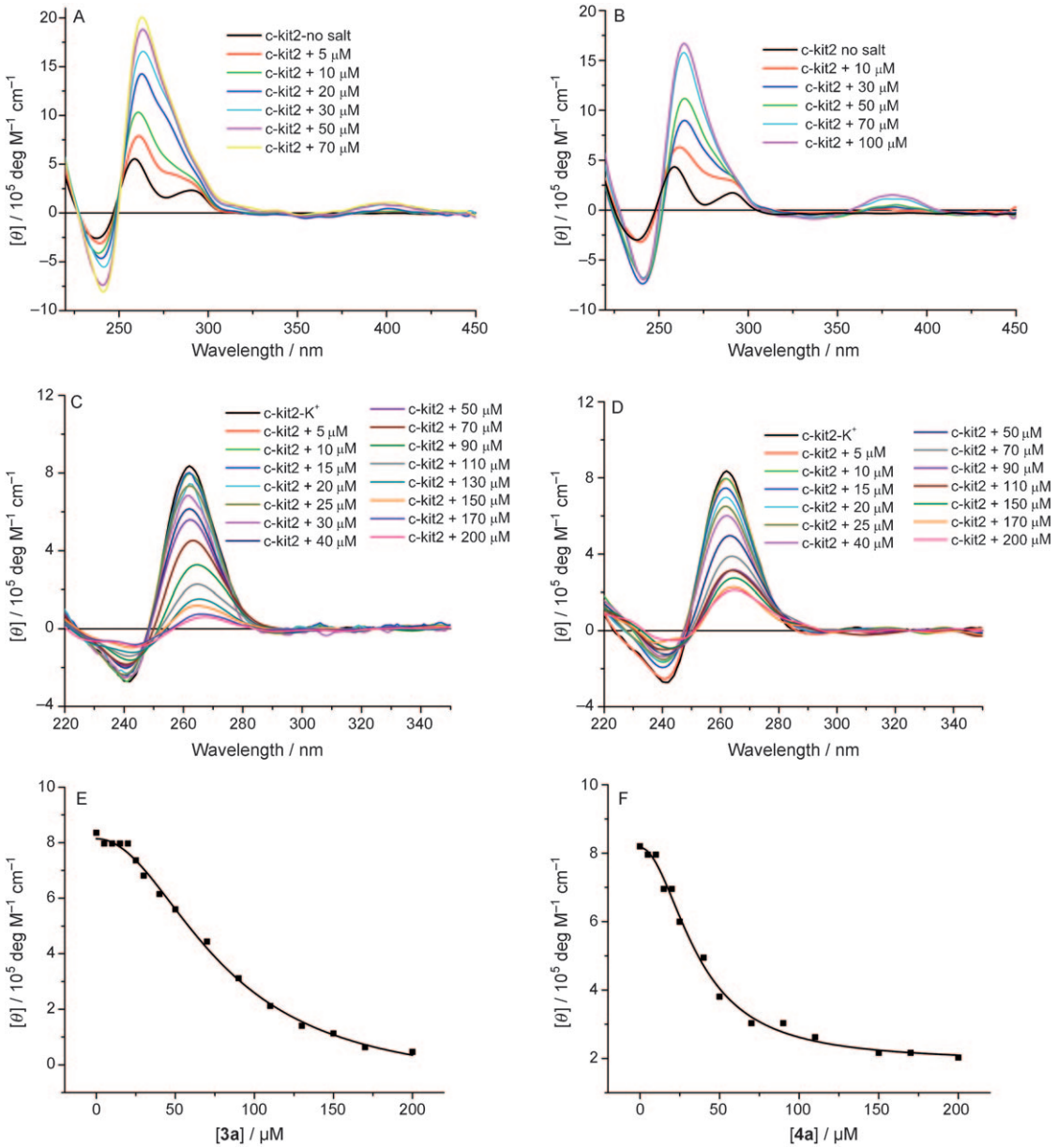

Figure 3. CD spectra of titration experiments of ligands **3a** (A) and **4a** (B) in the absence of added salt and ligands **3a** (C) and **4a** (E) in the presence of K^+ with c-kit2 G-quadruplex (10 μM); CD plots of molar ellipticity of c-kit2 against the concentration of ligands **3a** (E) and **4a** (F) in the presence of K^+ (the solid line represents the Hill 1 fitting).

260 nm, with the concomitant disappearance of the signal at 295 nm. Thus, ligand **3a** and **4a** appear to induce the formation of a single parallel conformation of the c-kit2 quadruplex (Figure 3). In the CD spectroscopic analysis with c-kit2 (Figure 3), besides the ligand-dependent increase in ellipticity at 260 nm we also observed the appearance of a relatively weak signal at 399 nm for ligand **3a** and 380 nm for ligand **4a**. This is indicative of a change in the chirality of the proximal chemical environment of ligand **3a** and **4a**.

In the presence of K^+ the c-kit2 quadruplex exists predominantly as a parallel structure (as indicated by a major positive peak at 260 nm and a minor peak at 240 nm), and we have reported that ligand **2** induced CD spectral changes were less prominent.[9b] We have observed a slight increase in ellipticity at 260 nm (that of the parallel structure) and an induced CD band at 380 nm of ligand **2**. We performed real-time titrations of ligands **3a** and **4a** into pre-annealed solutions of the G-quadruplex in buffer containing 100 mM KCl and 50 mM Tris·HCl at pH 7.4 (Figure 3C and D). Upon addition of ligand **3a** up to 25 μM (2.5 equiv) to the c-kit2 quadruplex there was no significant changes in ellipticity. However, upon titration of higher concentration of **3a**, the signal at 260 nm was found to decrease in a dose-dependent fashion until a point at ≈200 μM, beyond which no further reduction in the molar ellipticity was observed. The decrease in the CD signal suggested ligand-induced disruption

of the stacking between the bases of the G-quadruplex tetrads consistent with an apparent unfolding effect. This may be due to the ability of **3a** to recognise multiple binding sites at the higher concentration employed in the CD study.[4d] A similar but more pronounced effect was observed when **4a** was titrated into c-kit2. A plot of the molar ellipticity against the concentration of **3a** and **4a** gave a sigmoidal-shaped curve indicative of a cooperative effect, where the binding of **3a** and **4a** at one site increases the affinity for ligand binding at another site (Figure 3E and F).

Given that G-quadruplex DNA potentially has more than one binding site, we considered the possibility that ligands **3a** and **4a**, at higher concentrations, may bind at multiple sites and thus, start to remodel the secondary structure. By fitting the sigmoidal-shaped curves to the Hill 1 equation by using Origin 8.0 (see the Supporting Information), we obtained Hill coefficients (n) of 2.0 for binding of ligands **3a** and **4a** to c-kit2. This reveals that the binding of both ligands, **3a** and **4a**, exhibits positive cooperativity ($n>2$) for the c-kit2 quadruplex. Additionally, the concentrations of **3a** and **4a** that are required to reach 50% reduction of the molar ellipticity, $[D]_{50\%}$, for c-kit2 are estimated to be (78 ± 5) and (36 ± 2) μM, respectively. From the $[D]_{50\%}$ values, it is therefore possible to see that the cooperative effect is two-fold more pronounced for ligand **4a**.

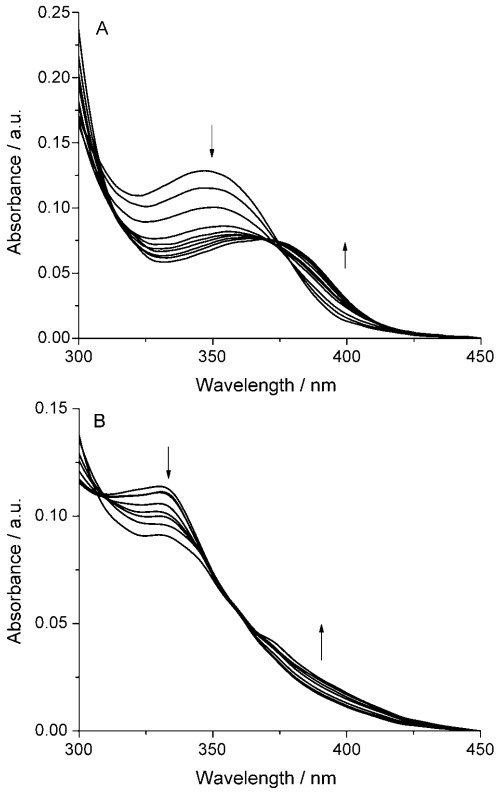

Figure 4. UV/Vis titration spectra of c-kit2 into a solution of ligands **3a** (A) and **4a** (B) in buffer solution containing KCl (100 mM) and Tris·HCl (10 mM) at pH 7.4.

UV/Vis binding titrations: We considered the possibility that **3a** and **4a** might first self-aggregate at high concentrations, which on binding could facilitate unfolding of the DNA secondary structure. UV/Vis absorption spectroscopy was used to investigate the DNA binding behaviour of ligands **3a** and **4a** with the c-kit2 quadruplex. UV/Vis experiments were performed in the presence of 10 μM of c-kit2 in buffer containing 100 mM KCl and 10 mM Tris·HCl at pH 7.4. The data obeyed the Beer–Lambert law and showed a linear correlation, indicating that ligand aggregation does not occur in the presence of DNA (see the Supporting Information). The binding affinities were calculated by sequential addition of aliquots of c-kit2 quadruplex DNA sample into ligand solutions, with absorbance spectra recorded after each addition. Ligand **3a** showed a strong absorbance at 260 nm and a peak at 350 nm. The UV/Vis spectra for ligand **4a** showed a strong absorption at 253 nm and a shoulder at 333 nm. The peaks at 253–260 nm overlap with the absorption peaks of the DNA and therefore, the binding affinities for the c-kit2 binding experiments were calculated by using the shoulders at 350 and 333 nm for ligands **3a** and **4a**, respectively (Figure 4A and B). UV/Vis absorption titration experiments show that the intensity of the band at 350 and 333 nm decreased with addition of G-quadruplex DNA. Interaction of ligands **3a** with c-kit2 produced up to 48% hypochromicity along with a red shift of up to 23 nm (Figure 4A), whereas there was only 16% hypochromicity along with a 6 nm shift of the band at 333 nm of ligand **4a** (Figure 4B). Both ligands show strong binding to the c-kit2 quadruplex ($K\cong10^7\,M^{-1}$) in agreement with the SPR results. The equilibrium binding constants K for ligands **3a** and **4a** calculated by using Equation (1) (see the Experimental Section and the Supporting Information) were $K=1.21\times10^7$ and $3.31\times10^7\,M^{-1}$, respectively.

Molecular modelling: Molecular modelling of ligand **3a** with the c-kit2 quadruplex (PDB entry: 2KQG) was performed by using two binding modes, the end-stacking and the groove-binding mode (Figure 5A, B and D). The docking results support that ligand **3a** - binds preferentially through the end-stacking mode (lower binding energy) to the c-kit2 quadruplex. The diethynyl–pyridine core stacks on the G-quartet with additional cation–dipole interaction of the pyridine nitrogen with the ion channel. These models also indicate that the 1,2,3-triazole heteroaromatic rings are positioned well for efficient π-stacking interactions with other bases of the c-kit2 G-quadruplex sequence allowing effective interaction of the side chains into the G-quadruplex grooves (Figure 5A, B and D). Ligand **4a** displays a similar stacking interaction with c-kit2 as shown in Figure 5C. The shorter side arms of ligand **4a**, when compared with **3a**, lead to a less pronounced interaction with the quadruplex loops, although it covers a larger surface area of the tetrad. This difference in interaction between the quadruplex and ligands **3a** and **4a**, respectively, could explain the smaller hypochromic shift observed in the UV/Vis titrations of c-kit2 with **4a** versus **3a**. Besides the end-stacking binding mode, the ligands might bind to the grooves of G-quadru-

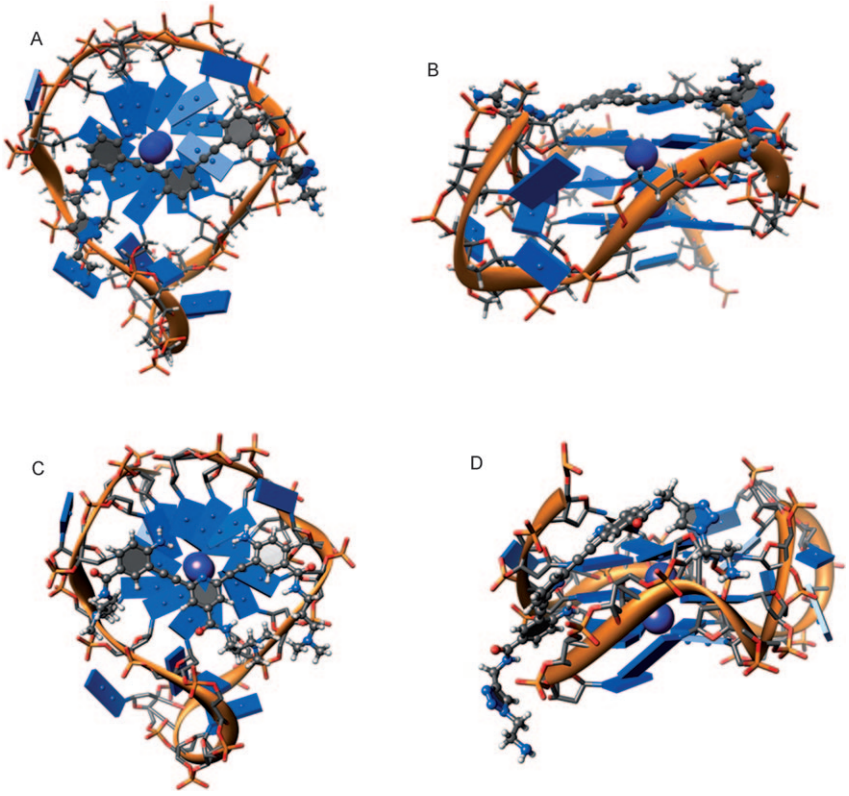

Figure 5. Amber99 force-field minimisation of the c-kit2 quadruplex with A) ligand **3a**, top view; B) ligand **3a**, side view, C) ligand **4a**, top view; and D) ligand **3a** binding to grooves of the c-kit2 quadruplex (1:1 stoichiometry).

plex DNA. The quadruplex DNA structures have different groove geometries and different patterns of donor–acceptor sites, which allows for these flexible ligands to display excellent structure-specific recognition, affinity and specificity.

Overall, ligands comprising triazole rings show better stabilisation and binding potential to G-quadruplexe DNA compared to ligand **2**. The observed selectivity may be due to the fact that ligands **3** have longer side chains each with at least one extra protonatable site (N atoms in triazole) and thus, **3** can interact better with the negatively charged phosphates of the quadruplexes. The selectivity of ligand **3** may also be due to the energy requirements for unfolding of the folded structure of triazole rings (see the Supporting Information) and the hydrogen-bonding potential of the side chains. Within the ligand series **3**, ligand **3c** with *N*,*N*-dimethylaminopropyl side chains (increasing chain length by one carbon atom over **3a** and **3b**), induces significant discrimination among intramolecular G-quadruplexes (binding ≈50-fold better to c-myc than k-ras and increasing the affinity by ≈40-fold for the c-kit1 over the k-ras quadruplex DNA). The small molecule series **4** with three protonated side chains incorporating amide groups was found to be a stronger G-quadruplex stabilising series compared to ligands **2** and **3**. This may be due to the electrostatic interactions between the positively charged molecules **4** and the anionic DNA target, and the hydrogen-bonding potential of the side chains. None of these ligands shows detectable binding to duplex DNA as observed by SPR, except ligand **4b** which shows some non-specific binding to duplex DNA (Figure 2 and the Supporting Information). The ligand-induced CD changes suggest that we cannot rule out the possibility that the quadruplex structure is being dynamically remodelled during the SPR experiments as has been observed by others.[17] The ligand–quadruplex complexes were investigated by molecular modelling, providing further information on structure–activity relationships.

Conclusion

We have designed and synthesised the 1,3-diethynyl-pyridine-based ligand series **3** and **4**. Ligands based on **3** were prepared by using copper(I)-catalysed click chemistry. We have studied the binding properties of the ligands with four distinct G-quadruplexes found in the promoter regions of the proto-oncogenes k-ras, c-myc and c-kit. These results reveal significant correlations between structural features and binding aptitudes of these ligands. Ligands of the trisubstituted series **4** were found to be strong stabilisers and tight binders. In general, all ligands in this study showed excellent selectivity for quadruplexes over duplex DNA and some diversity in G-quadruplex recognition with K_d (quadruplex) values varying from 120 nM to 19 μM (2-fold to 50-fold specificity). The biological properties of these small molecules are currently under investigation and will be reported in due course.

Experimental Section

General: All starting materials were obtained from commercial suppliers and used as received. Solvents were purified by standard techniques.[18] Experiments were carried out under an inert atmosphere. ^{1}H NMR and ^{13}C NMR spectra were recorded at 500 and 125 MHz, respectively, by using a Bruker DRX 500 instrument. ^{1}H NMR spectra were recorded in deuterated solvents as detailed and at ambient probe temperature (300 K). Chemical shifts are reported in parts per million (ppm) and are referenced to the residual solvent peak. The following notations are used: singlet (s), doublet (d), triplet (t), quartet (q), multiplet (m), broad (br). Data are reported in the following manner: chemical shift (multiplicity, coupling constant if appropriate, integration). Signals are quoted as δ values in ppm and coupling constants (J) are reported in Hertz. Residual protonated solvent signals were used as internal standard (^{1}H NMR: $\delta(CHCl_3)=7.26$, $\delta((CH_3)_2SO)=2.50$, $\delta(CH_3OH)=3.31$, δ-

(H_2O) = 4.67 ppm and ^{13}C NMR: $\delta(CHCl_3) = 77.16$, $\delta((CH_3)_2SO) = 39.52$, $\delta(CH_3OH) = 49.00$ ppm). Assignments are based on chemical shifts and/or DEPT as well as COSY, NOESY spectra. Mass spectra were recorded on a Micromass Q-Tof (ESI) spectrometer.

Thin layer chromatography (TLC) was performed on Merck Kieselgel 60 F254 glass plates and visualised under UV light. Flash column chromatography (FC) was performed by using Merck Kieselgel 60 silica gel and distilled solvents. HPLC was performed by using a Varian Pursuit C18, 5μ column (250×21.2 mm) and a gradient elution with 0.1% TFA/MeCN and 0.1% TFA/H_2O (TFA = trifluoroacetic acid) at a flow rate of 12.0 mL min^{-1}.

General procedure for synthesis of ligands 3: A mixture of dicarboxylic acid **8**[9b] (397.0 mg, 1.0 mmol), EDC·HCl (814.1 mg, 4.24 mmol), HOBt (572.8 mg, 4.24 mmol), NMM (849.7 mg, 8.40 mmol) and propargylamine (275.0 mg, 5.0 mmol, 5 equiv) in DMF (10 mL) was stirred at RT for 10 h. The solvent was removed in vacuo and the residue was dissolved in water. The precipitate formed was filtered off, washed with water and diethyl ether to give crude product **9** (403.0 mg, 86%) as a dark brown solid, which was used for click reactions without further purification.

A mixture of crude amide **9** (1 equiv), the aryl azide **10** (5 equiv), sodium ascorbate (0.2 equiv) and $CuSO_4 \cdot 5H_2O$ (10 mol%) in H_2O/*t*BuOH (1:1) was stirred at RT for 12 h. Removal of the solvent in vacuo and purification by HPLC (Solvents: A = Acetonitrile (0.1% TFA), B = H_2O (0.1% TFA) afforded the corresponding products **3a**–**c**.

Ligand 3a: Yield: 87%; red oil; ^1H NMR (500 MHz, D_2O): $\delta = 7.63$ (s, 2H), 7.52 (s, 1H), 7.18 (s, 2H), 7.04 (s, 2H), 7.00 (s, 2H), 6.10 (s, 2H), 4.46 (t, $J = 5.6$ Hz, 4H), 3.98 (sbr, 4H), 3.30 ppm (t, $J = 5.7$ Hz, 4H); ^{13}C NMR (125 MHz, D_2O): $\delta = 167.7$ (s), 152.5 (s), 142.4 (d), 136.7 (s), 132.6 (d), 130.6 (d), 126.7 (d), 124.1 (d), 117.3 (s), 115.0 (s), 114.1 (d), 102.5 (s), 94.6 (s), 88.0 (s), 47.1 (t), 38.7 (t), 34.4 ppm (t); HRMS (ESI): *m/z* calcd for $C_{33}H_{33}N_{13}O_2$: 644.2958 $[M+H]^+$; found: 644.2944.

Ligand 3b: Yield: 83%; red oil; ^1H NMR (500 MHz, D_2O): $\delta = 7.82$ (s, 2H), 7.68 (t, $J = 8.4$ Hz, 1H), 7.39 (s, 2H), 7.24 (d, $J = 7.4$ Hz, 2H), 7.19 (d, $J = 8.5$ Hz, 2H), 6.32 (d, $J = 8.3$ Hz, 2H), 4.71–4.67 (m, 4H, merged with D_2O), 4.21 (s, 4H), 3.67 (t, $J = 5.9$ Hz, 4H), 3.56 (m, 4H), 3.01–2.95 (m, 4H), 2.04–1.96 (m, 4H), 1.88–1.80 ppm (m, 4H); ^{13}C NMR (125 MHz, D_2O): $\delta = 167.9$ (s), 152.5 (s), 145.4 (s), 137.3 (s), 132.7 (d), 130.4 (d), 126.9 (d), 124.1 (d), 120.9 (s), 114.3 (d), 103.0 (s), 94.1 (s), 88.5 (s), 54.6 (s), 53.5 (s), 46.1 (t), 34.6 (t), 22.5 ppm (t), one aromatic CH could not be unambiguously determined; HRMS (ESI): *m/z* calcd for $C_{41}H_{45}N_{13}O_2$: 752.3897 $[M+H]^+$; found: 752.3926.

Ligand 3c: Yield: 84%; red oil; ^1H NMR (500 MHz, D_2O): $\delta = 7.60$ (s, 2H), 7.48 (t, $J = 7.7$ Hz, 1H), 7.19 (s, 2H), 7.03 (d, $J = 7.4$ Hz, 2H), 6.99 (d, $J = 8.5$ Hz, 2H), 6.10 (d, $J = 8.5$ Hz, 2H), 4.22 (t, $J = 6.7$ Hz, 4H), 4.01 (s, 4H), 2.91–2.89 (m, 4H), 2.61 (s, 12H), 2.10–2.08 ppm (m, 4H); ^{13}C NMR (125 MHz, D_2O): $\delta = 167.6$ (s), 152.4 (s), 144.7 (s), 141.7 (d), 137.4 (s), 132.5 (d), 130.4 (d), 126.5 (d), 123.7 (d), 120.4 (d), 113.9 (d), 102.9 (s), 93.5 (s), 88.6 (s), 54.3 (t), 46.9 (t), 42.5 (q), 24.5 ppm (t), one aromatic carbon could not be unambiguously determined; HRMS (ESI): *m/z* calcd for $C_{39}H_{45}N_{13}O_2$: 728.3897 $[M+H]^+$; found: 728.3920.

Triester derivative 13: A mixture of iodoaniline derivative **5** (544.0 mg, 2 mmol), diethynyl compound **12** (185.1 mg, 1 mmol), $[PdCl_2(PPh_3)_2]$ (70.2 mg, 10 mol%), and CuI (38 mg, 20 mol%) was evacuated and filled with argon. To the mixture DMF (10 mL) and triethylamine (2 mL) were added. After stirring at RT under an argon atmosphere for 9 h, the mixture was dried in vacuo. The residue was purified by chromatography on silica gel (EtOAc/hexane (1:1)→EtOAc) to afford **13** (353.0 mg,73%) as a light yellow solid. ^1H NMR (500 MHz, $CDCl_3$): $\delta = 8.14$ (d, $J = 2.0$ Hz, 2H), 7.98 (s, 2H), 7.84 (d, $J = 2.0$ Hz, 2H), 6.70 (d, $J = 8.6$ Hz, 2H), 4.90 (s, 4H), 4.00 (s, 3H), 3.87 ppm (s, 6H); ^{13}C NMR (125 MHz, $CDCl_3$): $\delta =$ 166.3 (s), 164.4 (s), 152.3 (s), 144.4 (s), 138.5 (s), 135.2 (d), 132.5 (d), 125.2 (d), 119.4 (s), 113.5 (d), 105.1 (s), 93.3 (s), 86.9 (s), 53.1 (q), 51.8 ppm (q); HRMS (ESI): *m/z* calcd for $C_{27}H_{21}N_3O_6$: 484.4721 $[M+H]^+$; found: 484.4742.

Triacid 14: To a solution of the methyl ester derivative **13** (100.0 mg) in methanol and THF (1:1, 10 mL) NaOH (5 mL, 2 N solution in water) was added at 0°C. After stirring for 12 h at RT, the solvents were removed in vacuo and the residue was dissolved in water and acidified with formic acid. The precipitate formed was collected by filtration and washed with water and diethyl ether to give the crude acid **14** (90.0 mg, 99%) as a light yellow solid, which was used without further purification. ^1H NMR (500 MHz, [D_6]DMSO): $\delta = 7.89$ (s, 2H), 7.69 (d, $J = 8.5$ Hz, 2H), 6.78 (d, $J = 8.5$ Hz), 6.53 (s, 2H), 4.91 (s, 4H), 3.33 ppm (s, 4H), the OH group could not be determined.

Preparation of ligand 4: A mixture of triacid **14** (0.25 mmol), EDC (1.06 mmol, 4.24 equiv), HOBt (1.06 mmol, 4.24 equiv), NMM (2.10 mmol, 8.40 equiv), amine **15** (0.78 mmol, 3.12 equiv) in DMF (5 mL) was stirred at RT overnight. The solvent was removed in vacuo and the residue was purified by HPLC (gradient: H_2O/MeCN (1% TFA) 20:80→MeCN (1% TFA) over 35 min, 12 mL min^{-1}) to give the desired compounds **4**.

Ligand 4a: Yield: 84%; reddish brown oil; ^1H NMR (500 MHz, D_2O): $\delta = 7.54$ (d, $J = 2.1$ Hz, 2H), 7.49 (s, 2H), 7.35 (dd, $J = 8.6$, 2.1 Hz, 2H), 6.58 (d, $J = 8.6$ Hz, 1H), 3.21 (t, $J = 6.9$ Hz, 4H), 3.16 (t, $J = 6.9$ Hz, 2H), 3.05–3.03 (m, 6H), 2.77 (s, 18H), 1.89–1.83 ppm (m, 6H); ^{13}C NMR (125 MHz, D_2O): $\delta = 168.9$ (s), 165.6 (s), 151.9 (s), 142.5 (s), 141.9 (s), 132.4 (d), 130.1 (d), 123.2 (d), 121.7 (s), 114.5 (d), 104.9 (s), 92.3 (s), 88.1 (s), 55.3 (t), 55.2 (t), 42.68 (q), 42.66 (q), 36.8 (t), 36.4 (t), 24.3 (t), 23.8 ppm (t); HRMS (ESI): *m/z* calcd for $C_{39}H_{51}N_9O_3$: 694.8905 $[M+H]^+$; found: 694.8916.

Ligand 4b: Yield: 81%; reddish brown oil; ^1H NMR (500 MHz, CD_3OD): $\delta = 7.75$ (s, 2H), 7.51 (d, $J = 2.1$ Hz, 2H), 7.49 (dd, $J = 8.7$, 2.1 Hz, 2H), 6.62 (d, $J = 8.7$ Hz, 2H), 3.33 (t, $J = 6.8$ Hz, 2H), 3.28 (t, $J =$ 6.7 Hz, 4H), 3.20-2.96 (m, 24H), 2.80 (t, $J = 7.2$ Hz, 4H), 2.75–2.72 (m, 2H), 2.69–2.68 (m, 9H), 1.81–1.76 ppm (m, 6H); ^{13}C NMR (125 MHz, $CDCl_3$): $\delta = 169.8$ (s), 166.7 (s), 155.1 (s), 145.2 (s), 144.8 (s), 133.8 (d), 131.4 (d), 124.6 (d), 122.4 (s), 114.8 (d), 104.9 (s), 92.2 (s), 89.3 (s), 55.7 (t), 55.6 (t), 53.5 (t), 53.1 (t), 50.9 (t), 50.8 (t), 43.7 (q), 43.6 (q), 38.6 (t), 37.9 (t), 26.5 (t), 26.4 ppm (t); HRMS (ESI): *m/z* calcd for $C_{48}H_{66}N_{12}O_3$: 859.5459 $[M+H]^+$; found: 859.5450.

FRET melting experiments: All DNA sequences tested were initially dissolved as a 100 μM stock solution in MilliQ (MQ) water. Further dilutions were carried out in 60 mM potassium cacodylate buffer, pH 7.4. Five dual fluorescently labelled DNA oligonucleotides were used in these experiments: k-ras was a dual-labelled 32-mer oligonucleotide comprising a quadruplex forming region in the promoter region of the human *k-ras* gene, 5′-FAM-AGG GCGGTG TGG GAA GAG GGA AGA GGG GGA GG-TAMRA; c-myc was a dual-labelled 22-mer oligonucleotide comprising one of the quadruplex forming regions in the promoter region of the human *c-myc* oncogene, 5′-FAM-TGA GGG TGG GTA GGG TGG GTA A-TAMRA-3′; c-kit1 was a dual-labelled 21-mer oligonucleotide comprising one of the quadruplex forming regions in the promoter region of the human *c-kit* oncogene, 5′-FAM-GGG AGG GCG CTG GGA GGA GGG-TAMRA-3′; c-kit2 was a dual-labelled 20-mer oligonucleotide comprising one of the quadruplex forming regions in the promoter region of the human *c-kit* oncogene, 5′-FAM-GGG CGG GCG CGA GGG AGG GG-TAMRA-3′; ds-DNA was a dual-labelled 20-mer oligonucleotide comprising a self-complementary sequence with a central polyethylene glycol linker able to fold into a hairpin, 5′-FAM-TAT AGC TAT A HEG TAT AGC TAT A-TAMRA-3′. The donor fluorophore was 6-carboxyfluorescein (FAM), and the acceptor fluorophore was 6-carboxytetramethylrhodamine, (TAMRA). Dual-labelled DNA was annealed at a concentration of 400 nM by heating at 94°C for 5 min followed by cooling to room temperature. One mM stock solution of ligands **3** and **4** were made up in MQ water. The 96-well plates (MJ Research, Waltham, MA) were prepared by aliquoting 50 μL of the annealed DNA into each well, followed by 50 μL of the compound solutions by using a Beckman Coulter liquid handling robot. Measurements were made in triplicate with an excitation wavelength of 483 nm and a detection wavelength of 533 nm by using a LightCycler 480 System RT-PCR machine (Roche). Final analysis of the data was carried out by using Origin Pro 7.5 data analysis and graphing software (OriginLab).

Surface plasmon resonance: Surface plasmon resonance measurements were performed on a four-channel BIAcore 3000 optical biosensor system (Biacore Inc.) by using a streptavidin-coated sensor chip (Biacore

SA-chip). We have used biotinylated G-quadruplex forming sequences; k-ras: d(biotin-[AGG GCG GGT GTG GGA AAG AGG GAA AGA GGG GGA GG], c-myc d(biotin-[TGA GGG TGG GTA GGG TGG GTA A]), c-kit1 d(biotin-[AGG GAG GGC GCT GGG AGG AGG G]), c-kit2 d(biotin-[CCC GGG CGG GCG CGA GGG AGG GGA GG]). We have also used a duplex DNA d(biotin-[GGG CAT AGT GCG TGG CGT TTA GC]) hybridised with its complementary sequence. The DNA oligonucleotides were folded in filtered and degassed running buffer (Tris·HCl 50 mM pH 7.4, 100 mM KCl; 95 °C for 5 min then cooled to room temperature overnight) and immobilised (≈500 RU except k-ras which was 2.5 times higher) in flow cells 2, 3 and 4, leaving the first flow cell empty as a blank. DNA binding experiments were carried out with running buffer at a flow rate of 20 μL min^{-1}. Solutions of ligands **3** and **4** were freshly prepared with running buffer by serial dilutions from stock solutions. These solutions were injected by using the KINJECT command (Biacore 3000 Control Software version 3.0.1) for 2 min followed by a 30 s 1 M KCl injection and a 30 s running buffer injection for chip regeneration. Each sample injection was repeated in duplicate. The response at equilibrium (R_{eq}) was plotted against the concentration of the analyte to generate a hyperbolic binding curve. The final graphs were obtained by subtracting blank sensorgrams from the duplex or quadruplex sensorgrams. Dissociation constants were determined by fitting the binding curve by using the steady state affinity algorithm (Biaevaluation 3.0.2).

UV spectroscopy: Absorption spectra were recorded on a Hitachi U-4100 UV/VIS-NIR spectrophotometer (for ligand **3a**) and a Cary 400 Bio UV/Vis spectrophotometer (for ligand **4a**) in the 200–450 nm range at 20 °C in 0.5 cm (ligand **4a**) and 1 cm (ligand **3a**) path length quartz cuvette. Aliquots of a concentrated solution of c-kit2 quadruplex ([GGGCGGGCGCGAGGGAGGGG] preannealed by heating at 95 °C for 5 min and then cooling to room temperature at 0.1 °C per minute in a buffer containing Tris·HCl (50 mM, pH 7.4) and KCl (100 mM) were added to ligands **3a** (30 μM) and **4a** (20 μM) and scanned immediately. Binding constants, K, were determined from a reciprocal plot of $D/\Delta\varepsilon_{ap}$ versus D, by using Equation (1).[19]

$$D/\Delta\varepsilon_{ap} = D/\Delta\varepsilon + 1/(\Delta\varepsilon \times K) \quad (1)$$

where $\Delta\varepsilon_{ap} = |\varepsilon_a - \varepsilon_f|$, $\Delta\varepsilon = |\varepsilon_b - \varepsilon_f|$, and ε_a, ε_f, and ε_b are the apparent, free and bound ligand extinctions, respectively. D is the DNA concentration. Binding constant K is then obtained by the ratio of the slope ($=1/\Delta\varepsilon$) and the y intercept ($=1/\Delta\varepsilon K$) from the linear fit of the reciprocal plot of $D/\Delta\varepsilon_{ap}$ versus D. The percent hypochromicity was calculated by using the percent hypochromicity $= \Delta\varepsilon/\varepsilon_f \times 100$.

Circular dichroism (CD): CD spectra were recorded on a JASCO J-815 spectrophotometer by using a 1 mm path length quartz cuvette. Quadruplex c-kit2 ([GGGCGGGCGCGAGGGAGGGG]) was annealed by heating at 95 °C for 5 min and then cooling to room temperature at 0.1 °C per minute in a buffer containing Tris·HCl (50 mM, pH 7.4) and KCl (100 mM). Aliquots of ligand **3a** and **4a** (1 mM in water) were added in steps to achieve the desired equivalent proportions. The CD spectra represent an average of three scans and were smoothed and zero corrected. Final analysis and manipulation of the data was carried out by using Origin 8.0.

Molecular modelling: Molecular modelling of the quadruplex–ligand interactions were performed by using the 2KQG (PDB entry) as the starting quadruplex structure and pre-optimised structures (PM3, 0.01 Kcal mol^{-1} Å^{-1}, convergence criterion) of **3b** and **4a**. The complexes were optimised by using the Amber99 force field with a continuous solvent model following the steepest descent algorithm (to 0.05 Kcal mol^{-1} Å^{-1}) and the Polak–Ribiere algorithm (to 0.01 Kcal mol^{-1} Å^{-1}). The resulting structures were placed in a "water box", thus minimising the structures in the presence of solvent specified at atomic level. These optimisations were carried out by using the OPLS force field to 0.05 Kcal mol^{-1} Å^{-1} convergence (see the Supporting Information).

Acknowledgements

We thank the BBSRC for project funding and also for a studentship (Z.A.E.W.), Cancer Research UK for program funding (S.B.) and European Commission (Marie Curie Incoming Postdoctoral Fellowship to J.D.) for funding. J.D. thanks CSIR India and G.D.P. thanks Pembroke College, Cambridge for funding. We thank Rabindra Nath Das for his help with the UV and CD titration experiments, Dr. Pravin Shirude is thanked for useful discussions relating to the FRET experiments and Dr. Chris Lowe for critical reading of the manuscript.

[1] a) A. M. Burger, F. Dai, C. M. Schultes, A. P. Reszka, M. J. B. Moore, J. A. Double, S. Neidle, *Cancer Res.* **2005**, *65*, 1489–1496; b) E. Mandine, J.-F. Riou, J.-L. Mergny, P. Mailliet, F. Boussin, *Oncogene* **2005**, *24*, 2917–2928; c) D. J. Patel, A. T. Phan, V. Kuryavyi, *Nucleic Acids Res.* **2007**, *35*, 7429–7455; d) Y. Qin, L. H. Hurley, *Biochimie* **2008**, *90*, 1149–1171; e) S. Neidle, G. N. Parkinson, *Biochimie* **2008**, *90*, 1184–1196; f) J.-H. Tan, L.-Q. Gu, J.-Y. Wu, *Mini-Rev. Med. Chem.* **2008**, *8*, 1163–1178; g) S. Balasubramanian, S. Neidle, *Curr. Opin. Chem. Biol.* **2009**, *13*, 345–353.

[2] a) A. K. Todd, M. Johnston, S. Neidle, *Nucleic Acids Res.* **2005**, *33*, 2901–2907; b) J. L. Huppert and S. Balasubramanian, *Nucleic Acids Res.* **2005**, *33*, 2908–2916; c) J. L. Huppert, S. Balasubramanian, *Nucleic Acids Res.* **2006**, *35*, 406–413.

[3] a) T. Simonsson, P. Pecinka, M. Kubista, *Nucleic Acids Res.* **1998**, *26*, 1167–1172; b) A. Siddiqui-Jain, C. L. Grand, D. J. Bearss, L. H. Hurley, *Proc. Natl. Acad. Sci. USA* **2002**, *99*, 11593–11598; c) A. T. Phan, V. Kuryavyi, H. Y. Gaw, D. J. Patel, *Nat. Chem. Biol.* **2005**, *1*, 167–173; d) N. Kumar, R. Basundra, S. Maiti, *Nucleic Acids Res.* **2009**, *37*, 103321–103331; e) R. K. Thakur, P. Kumar, K. Halder, A. Verma, A. Kar, J. L. Parent, R. Basundra, A. Kumar, S. Chowdhury, *Nucleic Acids Res.* **2009**, *37*, 172–183.

[4] a) H. Fernando, A. P. Reszka, J. Huppert, S. Ladame, S. Rankin, A. R. Venkitaraman, S. Neidle, S. Balasubramanian, *Biochemistry* **2006**, *45*, 7854–7860; b) S. Rankin, A. P. Reszka, J. Huppert, M. Zloh, G. N. Parkinson, A. K. Todd, S. Ladame, S. Balasubramanian, S. Neidle, *J. Am. Chem. Soc.* **2005**, *127*, 10584–10589; c) M. Bejugam, S. Sewitz, P. S. Shirude, R. Rodriguez, R. Shahid, S. Balasubramanian, *J. Am. Chem. Soc.* **2007**, *129*, 12926–12927; d) Z. A. E. Waller, S. A. Sewitz, S. T. Hsu, S Balasubramanian, *J. Am. Chem. Soc.* **2009**, *131*, 12628–12633.

[5] a) S. Cogoi, L. E. Xodo, *Nucleic Acids Res.* **2006**, *34*, 2536–2549; b) S. Cogoi, M. Paramasivam, B. Spolaore, L. E. Xodo, *Nucleic Acids Res.* **2008**, *36*, 3765–3780.

[6] For reviews, see: a) J. Cuesta, M. A. Read, S. Neidle, *Mini-Rev. Med. Chem.* **2003**, *3*, 11–21; b) D. Monchaud, M.-P. Teulade-Fichou, *Org. Biomol. Chem.* **2008**, *6*, 627–636.

[7] For specific recent examples, see; a) E. M. Rezler, J. Seenisamy, S. Bashyam, M.-Y. Kim, E. White, W. D. Wilson, L. H. Hurley, *J. Am. Chem. Soc.* **2005**, *127*, 9439–9447; b) A. De Cian, E. DeLemos, J.-L. Mergny, M.-P. Teulade-Fichou, D. Monchaud, *J. Am. Chem. Soc.* **2007**, *129*, 1856–1857; c) K. Shinohara, Y. Sannohe, S. Kaieda, K. Tanaka, H. Osuga, H. Tahara, Y. Xu, T. Kawase, T. Bando, H. Sugiyama, *J. Am. Chem. Soc.* **2010**, *132*, 3778–3782; d) S. G. Rzuczek, D. S. Pilch, A. Liu, L. Liu, E. J. LaVoie, J. E. Rice, *J. Med. Chem.* **2010**, *53*, 3632–3644.

[8] a) K. Jantos, R. Rodriguez, S. Ladame, P. S. Shirude, S. Balasubramanian, *J. Am. Chem. Soc.* **2006**, *128*, 13662–13663; b) A. Bugaut, K. Jantos, J.-L. Wietor, R. Rodriguez, J. K. M. Sanders, S. Balasubramanian, *Angew. Chem.* **2008**, *120*, 2717–2720; *Angew. Chem. Int. Ed.* **2008**, *47*, 2677–2680; c) Z. A. E. Waller, P. S. Shirude, R. Rodriguez, S. Balasubramanian, *Chem. Commun.* **2008**, 1467–1469; d) W. C. Drewe, R. Nanjunda, M. Gunaratnam, M. Beltran, G. N. Parkinson, A. P. Reszka, W. D. Wilson, S. Neidle, *J. Med. Chem.* **2008**, *51*, 7751–7767; e) S. Müller, G. D. Pantoş, R. Rodriguez, S. Balasubramanian, *Chem. Commun.* **2009**, 80–82; f) G. Collie, A. P. Reszka, S. M. Haider, V. Gabelica, G. N. Parkinson, S. Neidle, *Chem. Commun.* **2009**, 7482–7484.

[9] a) J. Dash, P. S. Shirude, S. Balasubramanian, *Chem. Commun.* **2008**, 3055–3057; b) J. Dash, P. S. Shirude, S.-T. D. Hsu, S. Balasubramanian, *J. Am. Chem. Soc.* **2008**, *130*, 15950–15956.
[10] a) H. C. Kolb, M. G. Finn, K. B. Sharpless, *Angew. Chem.* **2001**, *113*, 2056–2075; *Angew. Chem. Int. Ed.* **2001**, *40*, 2004–2021; b) H. C. Kolb, K. B. Sharpless, *Drug Discovery Today* **2003**, *8*, 1128–1137; c) J. E. Moses, A. D. Moorhouse, *Chem. Soc. Rev.* **2007**, *36*, 1249–1262.
[11] a) A. D. Moorhouse, A. M. Santos, M. Gunaratnam, M. Moore, S. Neidle, J. E. Moses, *J. Am. Chem. Soc.* **2006**, *128*, 15972–15973; b) W. C. Drewe, S. Neidle, *Chem. Commun.* **2008**, 5295–5297; c) J. E. Moses, D. J. Ritson, F. Zhang, C. M. Lombardo, S. Haider, N. Oldham, S. Neidle, *Org. Biomol. Chem.* **2010**, *8*, 2926–2930.
[12] J. M. Heemstra, J. S. Moore, *Org. Lett.* **2004**, *6*, 659–662.
[13] a) R. A. J. Darby, M. Sollogoub, C. McKeen, L. Brown, A. Risitano, N. Brown, C. Barton, T. Brown, K. R. Fox, *Nucleic Acids Res.* **2002**, *30*, 39e; b) A. De Cian, L. Guittat, M. Kaiser, B. Sacca, S. Amrane, A. Bourdoncle, P. Alberti, M.-P. Teulade-Fichou, L. Lacroix, J.-L. Mergny, *Methods* **2007**, *42*, 183–195.
[14] a) M.-P. Teulade-Fichou, C. Carrasco, L. Guittat, C. Bailly, P. Alberti, J.-L. Mergny, A. David, J.-M. Lehn, W. D. Wilson, *J. Am. Chem. Soc.* **2003**, *125*, 4732–4740; b) B. Nguyen, F. A. Tanious, W. D. Wilson, *Methods* **2007**, *42*, 150–161.
[15] a) S. Paramasivan, I. Rujan, P. H. Bolton, *Methods* **2007**, *43*, 324–331; b) P. Balagurumoorthy, S. K. Brahmachari, *J. Biol. Chem.* **1994**, *269*, 21858–21869; c) B. Jin, L. Gaffney, C. Wang, R. A. Jones, K. J. Breslauer, *Proc. Natl. Acad. Sci. USA* **1992**, *89*, 8832–8866.
[16] E. W. White, F. Tanious, M. A. Ismail, A. P. Reszka, S. Neidle, D. W. Boykin, W. D. Wilson, *Biophys. Chem.* **2007**, *126*, 140–153.
[17] K. Halder, S. Chowdhury, *Biochemistry* **2007**, *46*, 14762–14770.
[18] D. D. Perrin, W. L. F. Armarego, *Purification of Laboratory Chemicals*, 3rd ed., Pergamon Press, Oxford, **1988**.
[19] A. Wolfe, G. H. Shimer, Jr., T. Meehan, *Biochemistry* **1987**, *26*, 6392–6396.

Received: November 3, 2010
Published online: March 8, 2011

